PHYSICAL REVIEW A **84**, 063830 (2011)

Chirped femtosecond solitons and double-kink solitons in the cubic-quintic nonlinear Schrödinger equation with self-steepening and self-frequency shift

Alka, Amit Goyal, Rama Gupta, and C. N. Kumar
Department of Physics, Panjab University, Chandigarh 160 014, India

Thokala Soloman Raju*
Department of Physics, Karunya University, Coimbatore 641 114, India
(Received 1 October 2011; published 13 December 2011)

We demonstrate that the competing cubic-quintic nonlinearity induces propagating solitonlike dark(bright) solitons and double-kink solitons in the nonlinear Schrödinger equation with self-steepening and self-frequency shift. Parameter domains are delineated in which these optical solitons exist. Also, fractional-transform solitons are explored for this model. It is shown that the nonlinear chirp associated with each of these optical pulses is directly proportional to the intensity of the wave and saturates at some finite value as the retarded time approaches its asymptotic value. We further show that the amplitude of the chirping can be controlled by varying the self-steepening term and self-frequency shift.

DOI: 10.1103/PhysRevA.84.063830 PACS number(s): 42.81.Dp, 42.65.Tg

I. INTRODUCTION

The nonlinear Schrödinger equation (NLSE) in its many versions has various applications in different fields such as nonlinear optics [1], Bose-Einstein condensates [2], and biomolecular dynamics [3]. In nonlinear optics, the NLSE describes the dynamics of picosecond pulses that propagate in nonlinear media due to the delicate balance between group-velocity dispersion (GVD) and Kerr nonlinearity. However, over the past several years, ultrashort (femtosecond) pulses have been extensively studied due to their wide applications in many different areas such as ultrahigh-bit-rate optical communication systems, ultrafast physical processes, infrared time-resolved spectroscopy, and optical sampling systems [4]. To produce ultrashort pulses, the intensity of the incident light field increases, which leads to non-Kerr nonlinearities, changing the physical feature of the system. The dynamics of such systems should be described by the NLSE with higher-order terms such as third-order dispersion, self-steepening, and self-frequency shift [5,6]. Moreover, in some physical situations cubic-quintic nonlinear terms arise [7,8], due to non-Kerr nonlinearities, from a nonlinear correction to the refractive index of a medium. In general, unlike the NLSE, these models with non-Kerr effects are not completely integrable and cannot be solved exactly by the inverse scattering transform method [9]. Hence, they do not have soliton solutions; however, they do have solitary-wave solutions, which are often called solitons.

The effect of third-order dispersion is significant for femtosecond pulses when the GVD is close to zero. However, it can be neglected for pulses whose width is of the order of 100 fs or more, having power of the order of 1 W and GVD far away from zero [10]. However, the effects of self-steepening and self-frequency shift terms are still dominant and should be retained. Under these conditions, we have considered the higher-order NLSE with cubic-quintic nonlinearity of the form

$$i\psi_z + a_1\psi_{tt} + a_2|\psi|^2\psi + a_3|\psi|^4\psi + ia_4(|\psi|^2\psi)_t + ia_5\psi(|\psi|^2)_t = 0, \tag{1}$$

where $\psi(z,t)$ is the complex envelope of the electric field, a_1 is the parameter of GVD, a_2 and a_3 represent cubic and quintic nonlinearities, respectively, a_4 is the self-steepening coefficient, and a_5 is the self-frequency shift coefficient. For Eq. (1), many restrictive special solutions of the bright and dark types have been obtained [11,12]. Scalora *et al.* [13] used the model in Eq. (1), for $a_5 = 0$, to describe pulse propagation in a negative-index material, where the sign of GVD can be positive or negative.

Much of the work has been done on chirped pulses because of their application in pulse compression or amplification and thus they are particularly useful in the design of fiber-optic amplifiers, optical pulse compressors, and solitary-wave-based communications links [14,15]. The pulse with linear chirp and a hyperbolic-secant-amplitude profile was investigated numerically by Hmurcik and Kaup [16]. Subsequently, many authors have reported the existence of chirped solitonlike solutions [15,17,18]. One of the present authors solved Eq. (1) for $a_3 = 0$ and obtained solitonlike solutions with nonlinear chirp [10,19]. In this paper we consider the effect of quintic non-Kerr nonlinearity and obtain soliton solutions with a different form of chirping. We find that for certain parameter conditions between quintic, self-steepening, and self-frequency shift terms, the solutions will resemble NLSE solitons with velocity selection. We also report herein the existence of double-kink-type solitons with nonlinear chirp for Eq. (1). In all these cases, chirping varies as directly proportional to the intensity of the wave and saturates at some finite value as $t \to \pm\infty$. Further, we show that the amplitude of chirping can be controlled by varying the self-steeping and self-frequency shift terms. It is also shown that for the same values of all parameters, the equation can have either

*soloman@karunya.edu

dark(bright) solitons or double-kink-type solitons, depending upon the velocity and other parameters of the wave.

II. CHIRPED SOLITONLIKE SOLUTIONS

Here we are interested in finding chirped solitonlike solutions of Eq. (1). Hence we choose the following form for the complex envelope traveling-wave solutions:

$$\psi(z,t) = \rho(\xi)e^{i[\chi(\xi)-kz]}, \quad (2)$$

where $\xi = t - uz$ is the traveling coordinate and ρ and χ are real functions of ξ. Here $u = 1/v$, with v the group velocity of the wave packet. The corresponding chirp is given by $\delta\omega(t,z) = -\frac{\partial}{\partial t}[\chi(\xi) - kz] = -\chi'(\xi)$. Now, substituting Eq. (2) in Eq. (1) and separating out the real and imaginary parts of the equation, we arrive at the coupled equations in ρ and χ,

$$k\rho + u\chi'\rho - a_1\chi'^2\rho + a_1\rho'' - a_4\chi'\rho^3 + a_2\rho^3 + a_3\rho^5 = 0 \quad (3)$$

and

$$-u\rho' + a_1\chi''\rho + 2a_1\chi'\rho' + (3a_4 + 2a_5)\rho^2\rho' = 0. \quad (4)$$

To solve these coupled equations, we choose the ansatz

$$\chi'(\xi) = \alpha\rho^2 + \beta. \quad (5)$$

Hence, chirping is given as $\delta\omega(t,z) = -(\alpha\rho^2 + \beta)$, where α and β denote the nonlinear and constant chirp parameters, respectively. Using this ansatz in Eq. (4), we get the relations

$$\alpha = -\frac{3a_4 + 2a_5}{4a_1}, \quad \beta = \frac{u}{2a_1}. \quad (6)$$

Hence, the value of the chirp parameter depends on different coefficients of the evolution equation (1) such as diffraction, self-steepening, and self-frequency shift. This means that the amplitude of chirping can be controlled by varying these coefficients. Now using Eqs. (5) and (6) in Eq. (3), we obtain

$$\rho'' + b_1\rho^5 + b_2\rho^3 + b_3\rho = 0, \quad (7)$$

where $b_1 = \frac{1}{16a_1^2}[16a_1a_3 - (2a_5 + 3a_4)(2a_5 - a_4)]$, $b_2 = \frac{1}{2a_1^2}(2a_1a_2 - ua_4)$, and $= b_3 = \frac{1}{4a_1^2}(4ka_1 + u^2)$.

This elliptic equation is known to admit a variety of solutions such as periodic, kink, and solitary-wave-type solutions. In general, all traveling-wave solutions of Eq. (7) can be expressed in a generic form by means of the Weierstrass $\wp$ function [20]. In this paper we report various localized solutions for different parameter conditions. It is interesting to note that if $b_1 = 0$, i.e., the quintic term is related to self-steepening and self-frequency shift terms, then Eq. (7) reduces to a cubic nonlinear equation that admits dark and bright solitons. For the case when $b_2 = 0$, it can be solved for localized solutions by using a fractional transformation. For $b_3 = 0$, we show that the equation has a Lorentzian-type solution. In the most general case, when all the coefficients have nonzero values, Eq. (7) can be mapped onto a ϕ^6 field equation to obtain double-kink-type [21] and bright- and dark-soliton solutions [22] of Eq. (1).

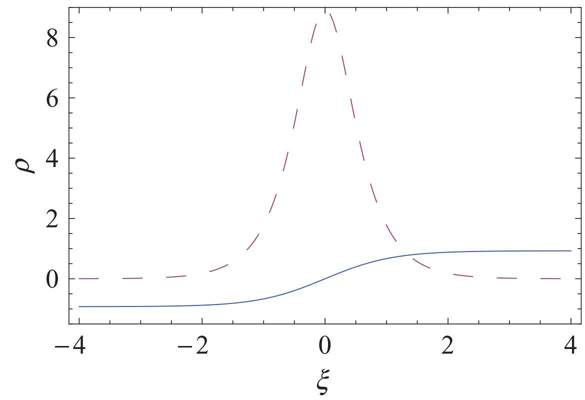

FIG. 1. (Color online) Amplitude profile for the (a) dark soliton (solid line) for $u = 4.1184$ and $k = 0$ and (b) bright soliton (dashed line) for $u = -30.1280$ and $k = -150.2856$.

In the following we delineate the parameter domains in which solitonlike solutions exist for this model. For example, when $b_1 = 0$ two interesting cases emerge that yield exact soliton solutions. (a) For $b_2 < 0$ and $b_3 > 0$, which implies $u > \frac{2a_1a_2}{a_4}$ and $k > \frac{-u^2}{4a_1}$, one obtains a dark-soliton solution of Eq. (1) of the form

$$\psi(z,t) = \sqrt{-\frac{b_3}{b_2}}\tanh\left(\sqrt{\frac{b_3}{2}}(t - uz)\right)e^{i[\chi(\xi)-kz]}. \quad (8)$$

The corresponding chirping is given by

$$\delta\omega(t,z) = \frac{\alpha b_3}{b_2}\tanh^2\left(\sqrt{\frac{b_3}{2}}\xi\right) - \beta. \quad (9)$$

(b) For $b_2 > 0$ and $b_3 < 0$, which implies $u < \frac{2a_1a_2}{a_4}$ and $k < \frac{-u^2}{4a_1}$, one can find a bright-soliton solution of the form

$$\psi(z,t) = \sqrt{-\frac{2b_3}{b_2}}\text{sech}[\sqrt{-b_3}(t - uz)]e^{i[\chi(\xi)-kz]}, \quad (10)$$

for which the chirping will be

$$\delta\omega(t,z) = \frac{2\alpha b_3}{b_2}\text{sech}^2(\sqrt{-b_3}\xi) - \beta. \quad (11)$$

Hence, the parametric condition $b_1 = 0$ implies that $16a_1a_3 = (2a_5 + 3a_4)(2a_5 - a_4)$ and the amplitude profile will be the

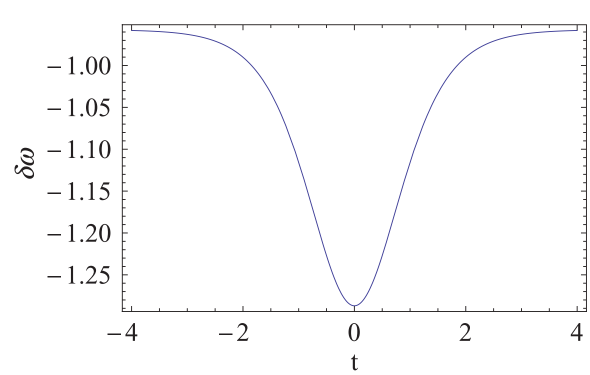

FIG. 2. (Color online) Chirping profile for the dark soliton plotted in Fig. 1.

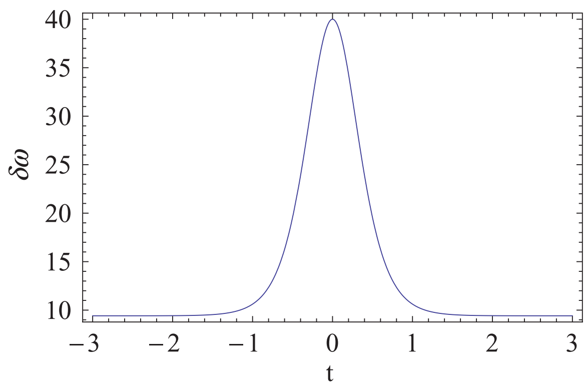

FIG. 3. (Color online) Chirping profile for the bright soliton plotted in Fig. 1.

same as for the NLSE, except the chirping will show nonlinear behavior. However, unlike for the NLSE, both dark and bright solitons exist in the normal and anomalous dispersion regimes. However, both soliton solutions have mutually exclusive velocity space. The amplitude profile of a typical dark and bright soliton is shown in Fig. 1, using the following values for the model parameters: $a_1 = 1.6001, a_2 = -2.6885, a_4 = 0.308\,14$, and $a_5 = 0.766\,04$. As $b_1 = 0$, the quintic-term coefficient is $a_3 = 0.1174$. The corresponding chirping for dark and bright solitons is shown in Figs. 2 and 3, respectively (for $z = 0$). It is clear from the figure that chirping for the dark soliton has a minimum at the center of the pulse, whereas for the bright soliton it has a maximum; however, for both cases it saturates at the same finite value as $t \to \pm\infty$.

III. CHIRPED FRACTIONAL-TRANSFORM SOLITONS

For the parametric condition $b_2 = 0$, we obtain very interesting chirped fractional-transform soliton. To accomplish this we now substitute $\rho^2 = y$ in Eq. (7), which can then be reduced to the following elliptic equation:

$$y'' + \tfrac{8}{3} b_1 y^3 + 4 b_3 y + c_0 = 0. \tag{12}$$

It is shown here that this elliptic equation connects to the well-known elliptic equation $f'' \pm af \pm bf^3 = 0$, where a and b are real, using a fractional transformation [23]

$$y(\xi) = \frac{A + Bf^2(\xi)}{1 + Df^2(\xi)}, \tag{13}$$

and we obtain the nontrivial Lorentzian-type solitons of Eq. (1).

Our main aim is to study the localized solutions: We consider the case where $f = \mathrm{cn}(\xi, m)$ with modulus parameter $m = 1$, which reduces $\mathrm{cn}(\xi)$ to $\mathrm{sech}(\xi)$. We can see that Eq. (13) connects $y(\xi)$ to the elliptic equation, provided $AD \neq B$, and the following conditions should be satisfied for the localized solution:

$$12 b_3 A + 8 b_1 A^3 + 3 c_0 = 0, \tag{14}$$

$$8 b_3 AD + 4 b_3 B + 4(B - AD) + 8 b_1 A^2 B + 3 c_0 D = 0, \tag{15}$$

$$4 b_3 AD^2 + 8 b_3 BD + 4(AD - B)D + 6(AD - B) + 8 b_1 AB^2 + 3 c_0 D^2 = 0, \tag{16}$$

$$12 b_3 BD^2 + 6(B - AD)D + 8 b_1 B^3 + 3 c_0 D^3 = 0. \tag{17}$$

From Eq. (15) we find that $D = \Gamma B$, where $\Gamma = \frac{4 + 4b_3 + 8b_1 A^2}{4A - 8b_3 A - 3c_0}$. Using this in Eq. (16), we determine B as

$$B = \frac{6(1 - A\Gamma)}{8 b_1 A + 4 b_3 \Gamma^2 A + 8 b_3 \Gamma + 4\Gamma(A\Gamma - 1) + 3 c_0 \Gamma^2}.$$

By substituting these expressions in Eqs. (14) and (17), we can determine A and c_0 for any given values of b_1 and b_3.

Thus, the localized solution is of the form

$$y(\xi) = \frac{A + B\,\mathrm{sech}^2(\xi)}{1 + D\,\mathrm{sech}^2(\xi)} \tag{18}$$

and $\rho(\xi)$ can be written as

$$\rho(\xi) = \sqrt{\frac{A + B\,\mathrm{sech}^2(\xi)}{1 + D\,\mathrm{sech}^2(\xi)}}. \tag{19}$$

The chirping takes the form

$$\delta\omega(t,z) = -\left[\alpha\left(\frac{A + B\,\mathrm{sech}^2(\xi)}{1 + D\,\mathrm{sech}^2(\xi)}\right) + \beta\right]. \tag{20}$$

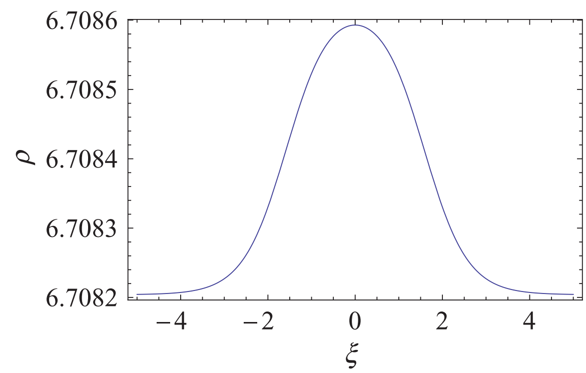

FIG. 4. (Color online) Typical amplitude profile for the soliton solution given by Eq. (19) for the values mentioned in the text.

The typical profiles for amplitude and chirping (for $z = 0$) are shown in Figs. 4 and 5, respectively, for $a_1 = 1.6001$, $a_2 = -2.6885$, $a_3 = 0.0260$, $a_4 = 0.308\,14$, $a_5 = 0.766\,04$, and $k = 0$. To make $b_2 = 0$, we set $u = -27.9215$.

In the following, we obtain yet another interesting algebraic soliton for the parametric condition $b_3 = 0$. In particular, for

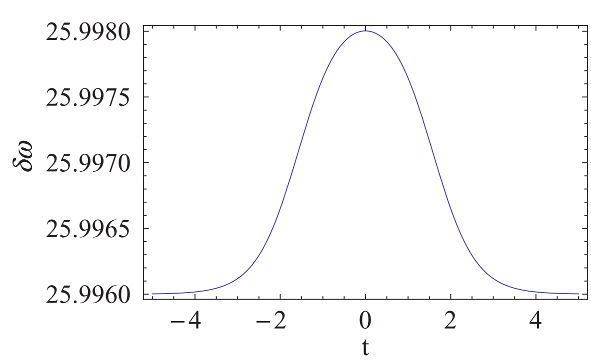

FIG. 5. (Color online) Chirping profile for the soliton solution plotted in Fig. 4.

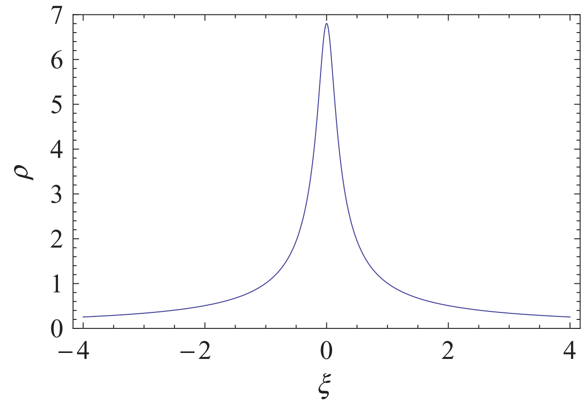

FIG. 6. (Color online) Typical amplitude profile for the soliton solution given by Eq. (21) for the values mentioned in the text.

$b_2 < 0$ and $b_1 > 0$, the solution of Eq. (7) is of the following form:

$$\rho(\xi) = \frac{1}{\sqrt{M + N\xi^2}}, \tag{21}$$

where $M = \frac{-2b_1}{3b_2}, N = \frac{-b_2}{2}$, and the chirping is given by

$$\delta\omega(t,z) = -\left(\frac{\alpha}{M + N\xi^2} + \beta\right). \tag{22}$$

For this case, the typical profiles for the amplitude and chirping (for $z = 0$) are shown in Figs. 6 and 7, respectively, for $a_1 = 1.6001$, $a_2 = -2.6885$, $a_3 = 0.2174$, $a_4 = 0.308\,14$, $a_5 = 0.766\,04$, and $u = 4.1185$. For $b_3 = 0$, we set $k = -121.8064$.

IV. CHIRPED DOUBLE-KINK AND BRIGHT(DARK) SOLITONS

We now demonstrate the existence of double-kink solitons and bright(dark) solitons when all the parameters in Eq. (7) are nonzero, i.e., $b_1 \neq 0$, $b_2 \neq 0$, and $b_3 \neq 0$. For the general case, Eq. (7) can be solved for double-kink-type (usually called two-kink) soliton solutions of the form [21]

$$\rho(\xi) = \frac{p\sinh(q\xi)}{\sqrt{\epsilon + \sinh^2(q\xi)}}, \tag{23}$$

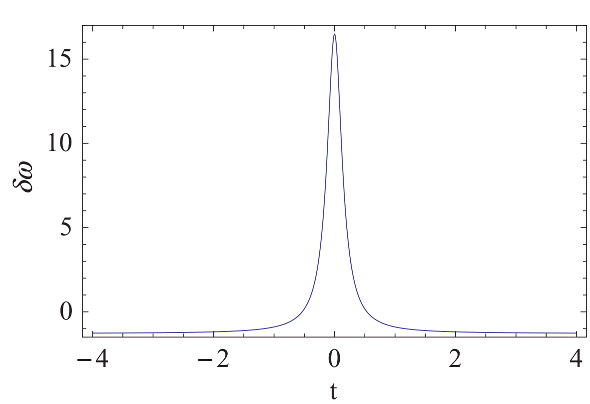

FIG. 7. (Color online) Chirping profile for the soliton solution plotted in Fig. 6.

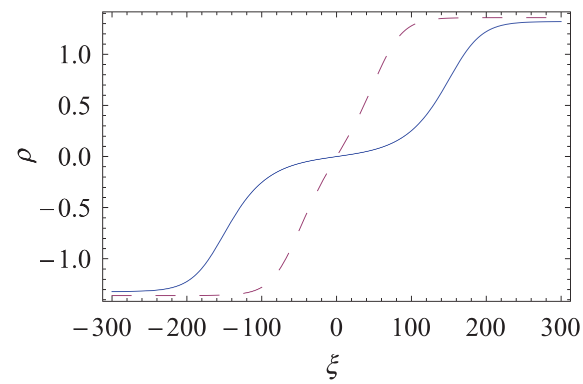

FIG. 8. (Color online) Typical amplitude profile of the soliton solution in Eq. (23) for different values of ϵ: $\epsilon = 1000$ for $p = 1.3204, q = 0.0252$, and $k = -141.911$ (solid line) and $\epsilon = 10$ for $p = 1.3584, q = 0.0287$, and $k = -141.899$ (dashed line).

where $b_1 = -\frac{3q}{p}(\frac{\epsilon-1}{\epsilon}), b_2 = 2pq(\frac{2\epsilon-3}{\epsilon})$, and $b_3 = -p^3q(\frac{\epsilon-3}{\epsilon})$. For this case, the chirping can be written as

$$\delta\omega(t,z) = -\left(\frac{\alpha p^2\sinh^2(q\xi)}{\epsilon + \sinh^2(q\xi)} + \beta\right). \tag{24}$$

The amplitude profile of the soliton solution for different values of ϵ is shown in Fig. 8 for $a_1 = 1.6001$, $a_2 = -2.6885$, $a_3 = 0.0260$, $a_4 = 0.308\,14$, $a_5 = 0.766\,04$, and $u = -30.1280$. The interesting double-kink feature of the solution given by Eq. (23) exists only for sufficiently large values of ϵ. One can also point out that as the value of ϵ changes, it effects only the width of the wave, but the amplitude of the wave remains the same. Chirping for the solution is shown in Fig. 9 (for $z = 0$), which has a minimum at the center of the pulse and saturates at the same finite value as $t \to \pm\infty$.

It is interesting to note that for $b_3 < 0$ and $b_2 > 0$, Eq. (7) has both bright and dark solitons depending on the value of b_1 [19]. The explicit solutions and corresponding chirping are given below.

If $b_1 < |\frac{3b_2^2}{16b_3}|$ then Eq. (7) has a bright-soliton-type solution, which is given as

$$\rho(\xi) = \frac{p}{\sqrt{1 + r\cosh q\xi}}, \tag{25}$$

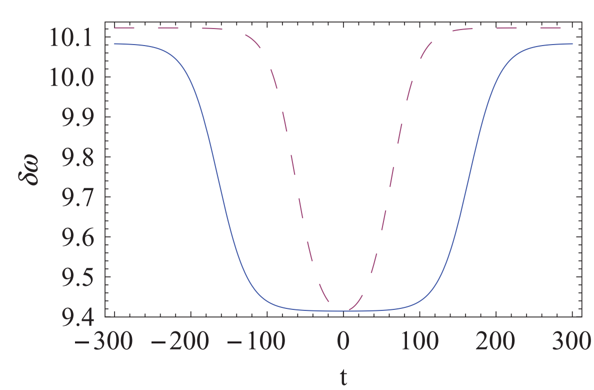

FIG. 9. (Color online) Chirping profile for the soliton solutions plotted in Fig. 8 for $\epsilon = 1000$ (solid line) and $\epsilon = 10$ (dashed line).

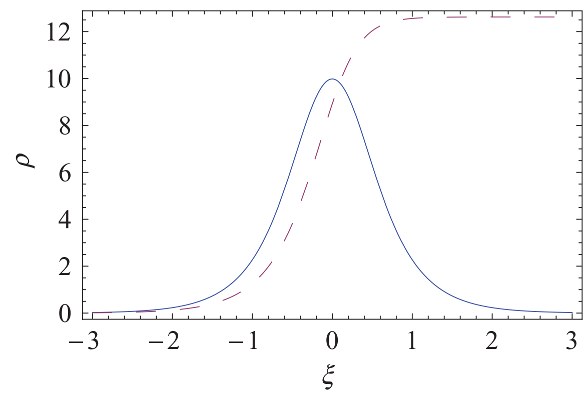

FIG. 10. (Color online) Amplitude profile of the soliton solutions in Eqs. (25) and (27) for $u = -30.1280$ and $k = -150.2856$: the bright soliton for $a_3 = 0.1168$ (solid line) and the dark soliton for $a_3 = 0.1164$ (dashed line).

where $p^2 = -\frac{4b_3}{b_2}, q^2 = -4b_3$, and $r^2 = 1 - \frac{16b_1b_3}{3b_2^2}$. The corresponding chirping is

$$\delta\omega(t,z) = -\left(\frac{\alpha p^2}{1 + r\cosh q\xi} + \beta\right). \tag{26}$$

If $b_1 = \frac{3b_2^2}{16b_3}$, then the solution of Eq. (7) will be of the dark-soliton type given by

$$\rho(\xi) = \pm p\sqrt{1 \pm \tanh q\xi}, \tag{27}$$

where $p^2 = -\frac{2b_3}{b_2}$ and $q^2 = -b_3$. For this case, the chirping is given as

$$\delta\omega(t,z) = -[\alpha p^2(1 \pm \tanh q\xi) + \beta]. \tag{28}$$

In Fig. 10 the amplitude profile of typical bright and dark solitons is shown for $a_1 = 1.6001$, $a_2 = -2.6885$, $a_4 = 0.308\,14$, and $a_5 = 0.766\,04$. It is interesting to note that Eq. (7) has bright and dark solitons depending on the value of the quintic-term coefficient, i.e., a_3, as shown in figure. It is shown that chirping (for $z = 0$) is also different in both cases: For a bright soliton chirping has maxima at the center of the pulse, which saturates at the same finite value (see Fig. 11), whereas for a dark soliton it saturates to different finite values as $t \to \pm\infty$. Hence, Eq. (7) has bright(dark) soliton

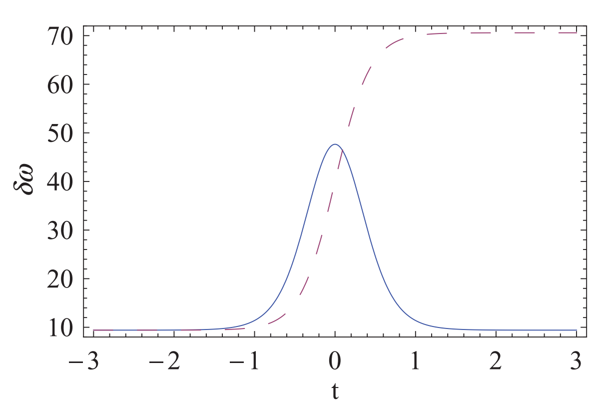

FIG. 11. (Color online) Chirping profile for the solitons plotted in Fig. 10: the bright soliton (solid line) and the dark soliton (dashed line).

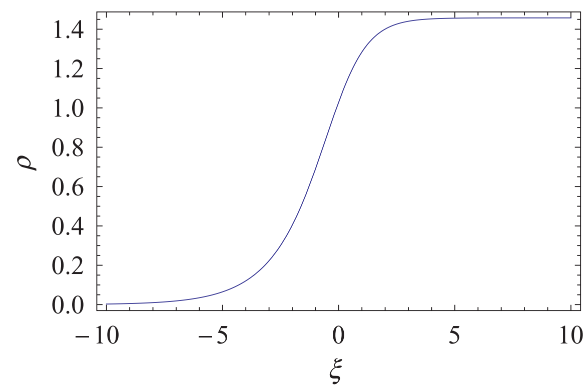

FIG. 12. (Color online) Amplitude profile of the soliton solution in Eq. (33) for $\gamma = 2.1245, \Delta = 0.2927$, and $k = -142.438$.

and double-kink-type soliton solutions for the same model parameters but for a different velocity selection and other parameters of the wave.

V. CHIRPED KINK SOLITONS FOR PURELY IMAGINARY a_5

Here we elucidate a more physically interesting case for which a_5 is imaginary in Eq. (1). Thus, for $a_5 \to ia_5$, Eqs. (3) and (4) read

$$k\rho + u\chi'\rho - a_1\chi'^2\rho + a_1\rho'' - a_4\chi'\rho^3 + a_2\rho^3 + a_3\rho^5 - 2a_5\rho^2\rho' = 0 \tag{29}$$

and

$$-u\rho' + a_1\chi''\rho + 2a_1\chi'\rho' + 3a_4\rho^2\rho' = 0. \tag{30}$$

Substituting Eq. (5) in Eq. (30), we obtain

$$\alpha = -\frac{3a_4}{4a_1}, \quad \beta = \frac{u}{2a_1}. \tag{31}$$

Now using Eqs. (5) and (31) in Eq. (29), we obtain

$$\rho'' + b_1\rho^5 + b_2\rho^3 + b_3\rho + b_4\rho^2\rho' = 0, \tag{32}$$

where $b_1 = \frac{1}{16a_1^2}(16a_1a_3 + 3a_4^2)$, $b_2 = \frac{1}{2a_1^2}(2a_1a_2 - ua_4)$, $b_3 = \frac{1}{4a_1^2}(4ka_1 + u^2)$, and $b_4 = -\frac{2a_5}{a_1}$. Equation (32) can be solved for a kink-type soliton solution of the form

$$\rho(\xi) = \sqrt{\frac{\Delta}{2}}\sqrt{1 + \tanh(\gamma\Delta\xi)}, \tag{33}$$

where $\gamma = \frac{b_4 \pm \sqrt{b_4^2 - 12b_1}}{6}, \Delta = \frac{b_2}{4\gamma^2 - b_4\gamma}$, and b_3 satisfies the condition that $b_3 = -\gamma^2\Delta^2$. The chirping is given by

$$\delta\omega(t,z) = -\left[\frac{\alpha\Delta}{2}[1 + \tanh(\gamma\Delta\xi)] + \beta\right]. \tag{34}$$

The amplitude profile of the soliton solution for different values of ϵ is shown in Fig. 12 for $a_1 = 1.6001$, $a_2 = -2.6885$, $a_3 = 0.0260$, $a_4 = 0.308\,14$, $a_5 = 0.766\,04$, and $u = -30.1280$. Chirping for this kink-type solution (depicted in Fig. 13) saturates to different finite values as $t \to \pm\infty$.

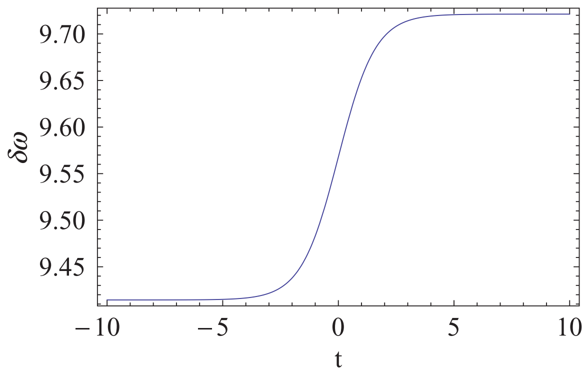

FIG. 13. (Color online) Chirping profile for the soliton solution plotted in Fig. 12.

VI. CONCLUSION

We would like to point out that the present work is a natural but significant generalization of Ref. [10] by considering the effect of competing cubic-quintic nonlinearity on the ensuing optical solitons in the higher-order nonlinear Schrödinger equation. We have demonstrated that the competing cubic-quintic nonlinearity induces propagating solitonlike dark(bright) solitons and double-kink solitons in the nonlinear Schrödinger equation with self-steepening and self-frequency shift. Parameter domains were delineated in which these optical solitons exist. In addition, fractional transform solitons were explored for this model. It was shown that the nonlinear chirp associated with each of these optical solitons is directly proportional to the intensity of the wave and saturates at some finite value as the retarded time approaches its asymptotic value. We have further shown that the amplitude of the chirping can be controlled by varying the self-steepening term and self-frequency shift. These optical solitons have nontrivial phase chirping that varies as a function of intensity and are different from that in Ref. [11], where the solution had a trivial phase. We hope that these chirped femtosecond solitons and double-kink solitons may be launched in long-distance telecommunication networks involving higher-order nonlinearities of the fiber.

ACKNOWLEDGMENT

A.G. and R.G. would like to thank CSIR, New Delhi, Government of India, for financial support through J.R.F. during the course of this work.

[1] A. Hasegawa, *Optical Solitons in Fibers* (Springer, Berlin, 1989).
[2] F. Dalfovo, S. Giorgini, L. P. Pitaevskii, and S. Stringari, Rev. Mod. Phys. **71**, 463 (1999).
[3] A. S. Davydov, *Solitons in Molecular Systems* (Reidel, Dordrecht, 1985).
[4] G. P. Agrawal, *Applications of Nonlinear Fiber Optics* (Academic, San Diego, 2001).
[5] Y. Kodama, J. Stat. Phys. **39**, 597 (1985).
[6] Y. Kodama and A. Hasegawa, IEEE J. Quantum Electron. **23**, 510 (1987).
[7] R. Radhakrishnan, A. Kundu, and M. Lakshmanan, Phys. Rev. E **60**, 3314 (1999).
[8] W. P. Hong, Opt. Commun. **194**, 217 (2001).
[9] M. J. Ablowitz and P. A. Clarkson, *Solitons, Nonlinear Evolution Equations and Inverse Scattering* (Cambridge University Press, New York, 1991).
[10] V. M. Vyas, P. Patel, P. K. Panigrahi, C. N. Kumar, and W. Greiner, Phys. Rev. A **78**, 021803(R) (2008).
[11] S. L. Palacios, A. Guinea, J. M. Fernandez-Diaz, and R. D. Crespo, Phys. Rev. E **60**, R45 (1999).
[12] Z. Li, L. Li, H. Tian, and G. Zhou, Phys. Rev. Lett. **84**, 4096 (2000).
[13] M. Scalora, M. S. Syrchin, N. Akozbek, E. Y. Poliakov, G. D'Aguanno, N. Mattiucci, M. J. Bloemer, and A. M. Zheltikov, Phys. Rev. Lett. **95**, 013902 (2005).
[14] M. Desaix, L. Helczynski, D. Anderson, and M. Lisak, Phys. Rev. E **65**, 056602 (2002).
[15] V. I. Kruglov, A. C. Peacock, and J. D. Harvey, Phys. Rev. Lett. **90**, 113902 (2003).
[16] L. V. Hmurcik and D. J. Kaup, J. Opt. Soc. Am. **69**, 597 (1979).
[17] S. Chen and L. Yi, Phys. Rev. E **71**, 016606 (2005).
[18] T. S. Raju, e-print arXiv:1107.2199.
[19] C. N. Kumar and P. Durganandini, Pramana—J. Phys. **53**, 271 (1999).
[20] E. Magyari, Z. Phys. B **43**, 345 (1981).
[21] N. H. Christ and T. D. Lee, Phys. Rev. D **15**, 1606 (1975).
[22] S. N. Behra and A. Khare, Pramana—J. Phys. **15**, 245 (1980).
[23] V. M. Vyas, T. S. Raju, C. N. Kumar, and P. K. Panigrahi, J. Phys. A **39**, 9151 (2006).